Effects of deuteron potentials on deuteron-induced nonelastic cross sections based on the intranuclear cascade model

Masahiro Nakano [1,*] Yuji Yamaguchi [2] and Yusuke Uozumi [3]

[1]*New Medical Statistics Research Institute, 1245-11 Tateiwa, Iizuka, Fukuoka 820-0003, Japan*
[2]*J-PARC Center, Japan Atomic Energy Agency, 2–4 shirakata, Tokai, Ibaraki 319-1195, Japan*
[3]*Department of Applied Quantum Physics and Nuclear Engineering, Kyushu University,
744 Motooka, Nishi-ku, Fukuoka 819-0395, Japan*

The aim of this paper is to investigate how the choice of deuteron potential affects the nonelastic cross sections of ^{12}C, ^{40}Ca, ^{58}Ni, and ^{208}Pb in the low-energy region below 200 MeV within the extended framework of the intranuclear cascade model, in which a three-body proton-neutron-target system is introduced to incorporate naturally the decomposition and capture reactions from weakly bound deuterons. To determine an appropriate potential for the two nucleons of the deuteron, we compare two phenomenological potentials with the Gaussian potential that we have used previously. Specifically, we examine the Reid and Coester-Yen soft-core potentials and find that they give reduced nonelastic cross sections. To investigate the role of the potential, we separate it into the tail region in the outer part and the soft-core region in the central part. By using a gluing method to connect the Gaussian potential smoothly to the Yukawa tail, we show that the tail has no appreciable effect for any of the targets. On the other hand, by adding a soft core to the ordinary Gaussian potential, we show that the soft core has appreciable effects, especially in heavier nuclei such as ^{208}Pb, the reason being the reduced breakup process with a soft-core potential from the deuteron rotation due to the Coulomb potential. The results of this study show that while the Yukawa tail has no appreciable effect, soft-core potentials tend to give reduced nonelastic cross sections, especially for heavy nuclei.

I. INTRODUCTION

Deuteron-induced nonelastic cross sections (sometimes called deuteron-induced total reaction cross sections) have been measured experimentally at incident energies below 200 MeV for ^{12}C, ^{40}Ca, ^{58}Ni, and ^{208}Pb as shown in Fig. 1. One may consider as a simple model that these experimental data of deuteron-induced reactions can be understood by simply assuming that the cross section is an independent sum of the proton-induced and neutron-induced nonelastic cross sections, each of which has half the energy of the incident deuteron. This sum is straightforward if experimental data for the corresponding nucleon-induced nonelastic cross sections exist, but sufficient data do not exist for ^{40}Ca and ^{58}Ni, so the missing data must be estimated by a well-fitting empirical formula.

Recently, we presented such a formula for proton-induced or neutron-induced nonelastic cross sections for arbitrary energy and general targets [1]. Despite being empirical, this general formula is based on the intranuclear cascade (INC) model [2,3] and so includes Coulomb and discrete-level-constraint effects [4], which play important roles in reproducing single-nucleon-induced nonelastic cross sections, especially at low energy. Using this formula for ^{12}C, ^{40}Ca,

^{58}Ni, and ^{208}Pb, the results of summing the proton-induced and neutron-induced nonelastic cross sections are shown by the dotted lines in Fig. 1, along with the corresponding experimental data.

Figure 1 shows that the simple summation overestimates the experimental values, especially for heavy target nuclei. The estimated values for ^{12}C are close to the experimental values because the radius of the deuteron (2.13 fm) is almost the same as that of ^{12}C (2.34 fm) according to Negele's formula [6], in which case the two nucleons in the incident deuteron are considered to be independent for a similarly sized target. In the other nuclei, the radii are 3.59, 4.04, and 6.52 fm for ^{40}Ca, ^{58}Ni, and ^{208}Pb, respectively, and now the cross-sectional area of the target is larger than the radius of the deuteron. The fact that the experimental values are smaller than the free sum of two nucleon contributions suggests that the finite-size potential between the two nucleons in the deuteron is important for heavy targets. Based on this idea, we have previously extended the INC model to include the mutual interaction between the two nucleons [7]. Also important is that the introduced mutual potential incorporates naturally the breakup and capture processes from weakly bound deuterons.

In our previous paper [7], the Gaussian potential was incorporated for the two deuteron nucleons, but in many quantum-mechanical applications, phenomenological soft-core potentials are often used to describe deuteron reactions [8–15]. Furthermore, it is considered realistic to use the
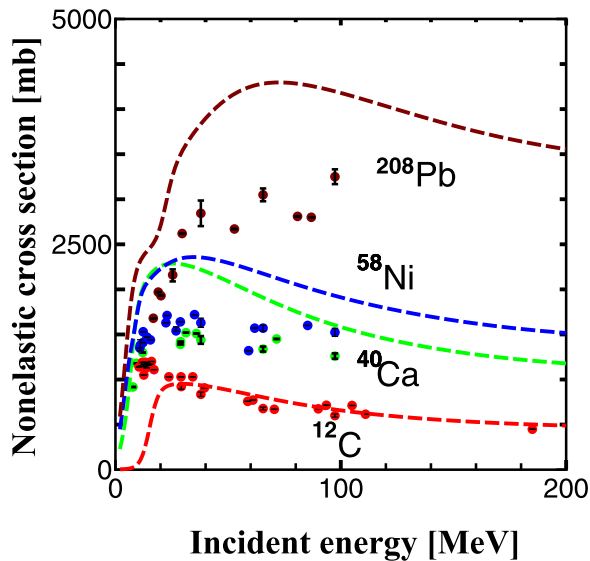
*nakano@med.uoeh-u.ac.jp

FIG. 1. Comparison of estimation by the simple model mentioned above (dashed lines) and experimental data (circles with error bars) for ^{12}C, ^{40}Ca, ^{58}Ni, and ^{208}Pb [5]. For the lighter nuclei, the error bars are smaller than the data points.

Yukawa tail for surface geometry due to pion exchange. Therefore, the aim of this paper is to investigate how the mutual potential affects deuteron-induced nonelastic cross sections. To advance the discussion, the analysis is performed as follows. First, taking the Reid and Coester-Yen soft-core potentials as specific examples, we show how realistic soft-core potentials differ from the Gaussian potential. Next, we investigate the origin of this difference by dividing the potential region into two parts: the surface region and the central region. To investigate the effects in the surface region, we compare the normal Gaussian potential with a merged potential that is converted smoothly from the original Gaussian potential to the Yukawa tail by means of a merging technique. To investigate the effects in the central region, we compare the original Gaussian potential and one with a soft core added to its central region.

II. INC MODEL AND GAUSSIAN POTENTIAL FOR DEUTERON

The original INC model has been shown to be advantageous for describing various phenomena such as pion, antiproton, and light-cluster injections [16–21], and the Uozumi group showed that the INC model combined with the generalized evaporation model [22] can explain double differential cross sections [23–27].

Here, we further extend the INC model to include the mutual potential in the deuteron [7]. In this INC model, we solve the time evolution of the three-body proton-neutron target system based on a relativistic many-body formalism with stochastic collisions, leading to explicit cross sections of different processes by assembling probabilistic processes. The time evolution is divided into two periods: before and after the nucleons in the deuteron collide with the target nucleons. The

precollision motion is determined uniquely by the classical equations of motion, while the postcollision motion follows a stochastic process according to the usual INC model. For the precollision motion, we introduce the following simple relativistic Hamiltonian:

$$H = \sum_i \sqrt{P_i^2 + m_i^2} + \sum_{ij} U_{ij}(i, j = 1, 2, 3), \quad (1)$$

where subscripts 1 and 2 indicate the proton and neutron, respectively, and subscript 3 indicates the target; therefore, p_1 and p_2 are the momenta of the proton and neutron, respectively, p_3 is the momentum of the center of mass of the target, and m_i is the corresponding masses. In the classical limit, this Hamiltonian becomes the ordinary Hamiltonian with rest mass, and the advantages of this form are that total energy and momentum are conserved and the deuteron splitting and nucleon capture by the potential can be discussed explicitly.

The potential U_{i3} is the sum of the nuclear potential in Woods-Saxon form and the Coulomb potential of finite-size charge distribution between nucleon and target, while the potential U_{12} is the deuteron mutual potential discussed in this paper. In a previous paper [7], we used a Gaussian-type phenomenological potential for the mutual potential of the two nucleons in the deuteron as shown in Refs. [28] and [29], where the Gaussian parameters have been fitted to the deuteron binding energy and $^3S_1$ phase shifts:

$$U_{12}(r) = V_0 \exp(-(r/b)^2), \quad \text{with} \quad r = |r_1 - r_2|/2, \quad (2)$$

where $V_0 = -72.15$ MeV and $b = 1.484$ fm.

In the initial stage, the two nucleons in the deuteron are placed at the z axis $Z_g \approx -500$ fm to include sufficiently the effect of the Coulomb potential, and the angle of the deuteron axis and the impact parameter are taken at random. While oscillating around the center of the deuteron, the two nucleons proceed to the target placed at the origin $Z_g = 0$ and then search for collisions with the nucleons in the target. Those collisions happen according to the nucleon-nucleon cross sections, the parameters of which are the same as those used in previous studies of nucleon-induced reactions in the INC model [2–4]. See Ref. [7] for more details about the extended INC model.

The results calculated in this way using the Gaussian potential are shown by the solid lines in Fig. 2. The satisfactory reproduction of the experimental values indicates the importance of introducing the finite-size potential of the deuteron instead of the free motions. Note that we obtained these results using the original potential parameters without adjusting them to reproduce the experimental data.

III. EFFECTS OF REALISTIC SOFT-CORE POTENTIALS

In this paper, we focus on two potentials with different depths and ranges, namely, the Reid [8] and Coester-Yen [9] soft-core potentials. Figure 3 shows the radial dependencies of triplet-even of these potentials together with that of the Gaussian potential that we used in a previous paper.

These soft-core potentials are thought to consist of a one-pion exchange potential in the outer region, a nuclear potential in the middle region created by not only 2π exchange but
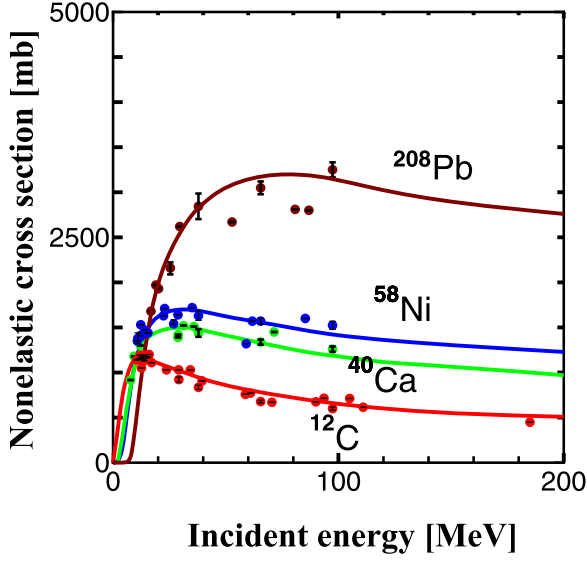
FIG. 2. Comparison between results obtained using extended INC model with Gaussian potential [7] (solid lines) and experimental data (circles with error bars) for ^{12}C, ^{40}Ca, ^{58}Ni, and ^{208}Pb.

also other meson exchanges such as σ, ω, and ρ mesons, and a phenomenologically repulsive core in the central part, which is thought to simulate the nuclear force resulting from antisymmetry between the quarks [30].

The nonelastic cross sections calculated using the extended INC model with the soft-core potentials are shown in Fig. 4 together with those calculated using the Gaussian potential. The effect of the soft-core potentials is noticeable for heavy nuclei such as ^{208}Pb in that they give smaller cross sections than does the Gaussian potential. By contrast, there is no appreciable effect for light nuclei below ^{58}Ni, and it is interesting that the difference between two soft-core potentials is not
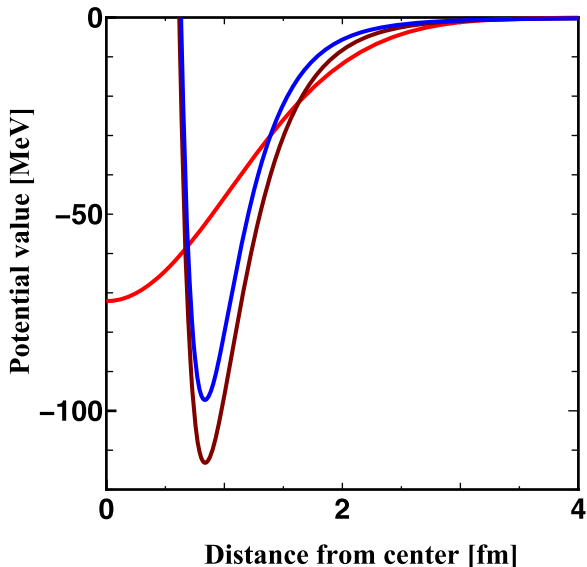

FIG. 3. Comparison of Coester-Yen (brown line) and Reid (blue line) soft-core potentials and original Gaussian potential (red line).
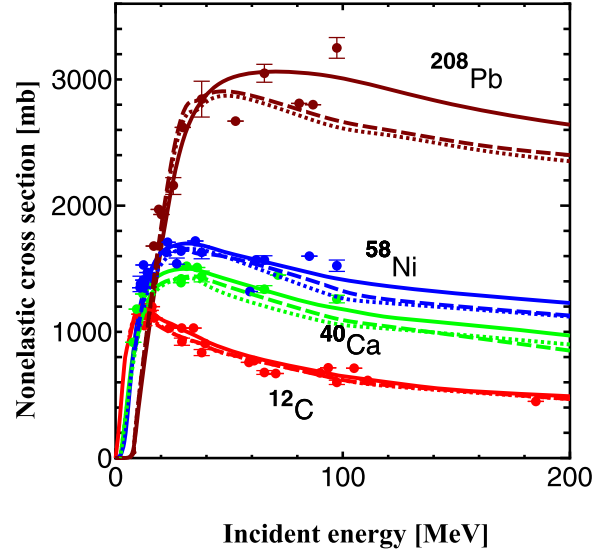

FIG. 4. Comparison of results obtained using Coester-Yen (dotted lines) and Reid (dashed lines) soft-core potentials and Gaussian potential (solid lines) for nonelastic cross sections of ^{12}C, ^{40}Ca, ^{58}Ni, and ^{208}Pb.

so important, since the shapes of the potentials are not very different.

IV. EFFECT OF YUKAWA TAIL

The soft-core potentials give smaller cross sections than does the Gaussian potential, especially for ^{208}Pb. We investigate the reason for this difference from two perspectives: the tail effect and the soft-core effect. First, we show the tail effect by changing from the Gaussian tail to the Yukawa tail without changing the Gaussian shape in the central region of the deuteron. For this, we use the method of the gluing of two potentials, which connects two arbitrary physical functions smoothly so that the merged function is differentiable everywhere.

A smooth function F that merges functions g and h at point $r_\mp$ is given by

$$F(r) = P_- g(r) + P_+ h(r), \qquad (3)$$

where

$$P_\mp = 1/\{1 + \exp[\pm(r - r_\mp)/w_\mp]\}. \qquad (4)$$

Here, the parameter $r_\mp$ is the gluing point and $w_\mp$ is the gluing range. The lower projection P_- is approximately unity when r is approximately zero and zero when r is large, and the upper projection P_+ has the opposite nature because $P_- + P_+ = 1$ when $r_- = r_+$ and $w_- = w_+$.

For our purpose, we take the Gaussian function for the central region and the Yukawa tail of the Reid soft-core potential for the outer region. Figure 5 shows the resulting merged potential, which changes gradually from the Gaussian potential in the central region to the Yukawa tail outside 1 fm. In this gluing, the gluing point $r_\mp$ is taken as the one-pion exchange range, that is, 1.413 fm, and the gluing width is taken as $w_\mp = 0.2$ fm to slowly change to the outer part of
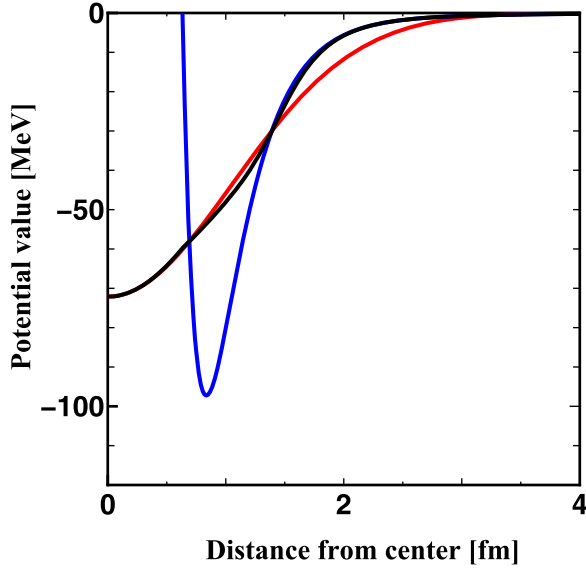
FIG. 5. Merged potential (black line) changes smoothly from Gaussian potential (red line) to Yukawa tail of Reid soft-core potential (blue line).

the Reid soft-core potential. Using this merged potential, the INC calculation gives the results as shown in Fig. 6, which shows clearly that the Yukawa tail does not play an important role in the nonelastic cross sections for any target below 200 MeV, although there is a small difference for ^{208}Pb.

V. GAUSSIAN SOFT-CORE POTENTIAL

In order to purely analyze the effect of the soft-core potential compared to the Gaussian potential, we set the following

schematic potential:

$$U_{12}^N(r) = V_0 \exp[-(r/b)^2] + V_{sc} \exp[-(r/b_{sc})^2], \quad (5)$$

where a soft core is added to the original Gaussian potential. The parameters of the soft-core part of the potential are chosen as $V_{sc} = 2000$ MeV and $b_{sc} = 0.32$ fm to reproduce that of the Coester-Yen potential as shown in Fig. 7, and we refer to this new potential as the Gaussian soft-core potential.

The nonelastic cross sections obtained using the Gaussian soft-core potential are shown in Fig. 8, which indicates

FIG. 7. Gaussian soft-core potential (black line) changes smoothly from Gaussian potential (red line) to potential with soft core. Shown for comparison is the Reid soft-core potential (blue line).
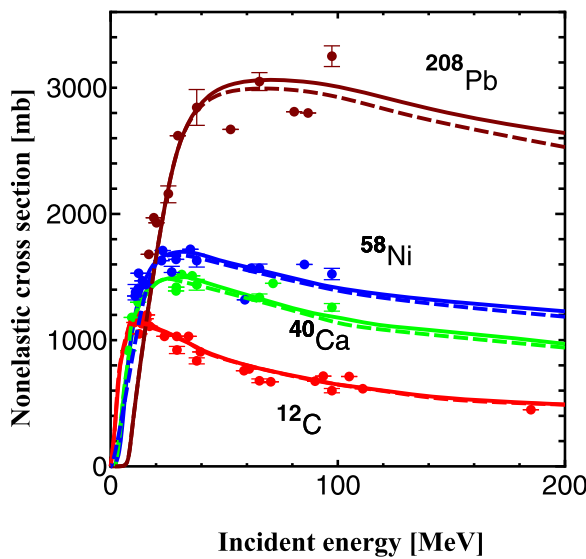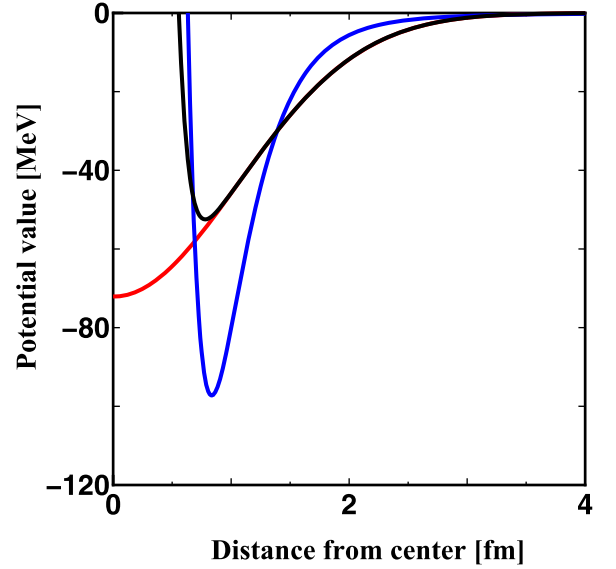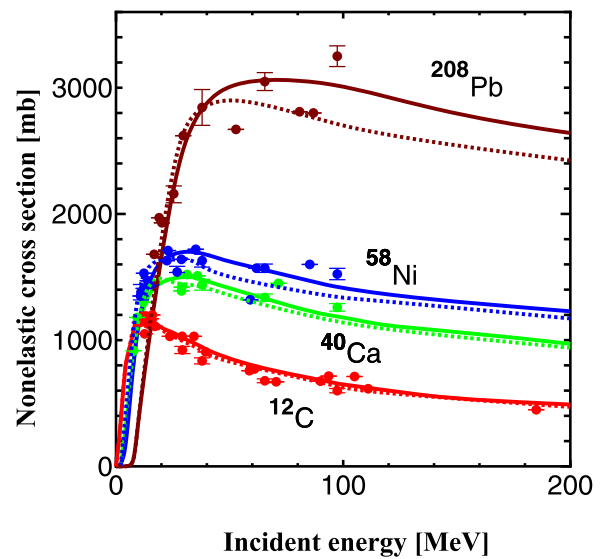

FIG. 6. Comparison of results obtained using merged potential (dashed lines) and original Gaussian potential (solid lines) for nonelastic cross sections of ^{12}C, ^{40}Ca, ^{58}Ni, and ^{208}Pb.

FIG. 8. Comparison of Gaussian soft-core potential (dashed lines) and original Gaussian potential (solid lines) for nonelastic cross sections of ^{12}C, ^{40}Ca, ^{58}Ni, and ^{208}Pb.
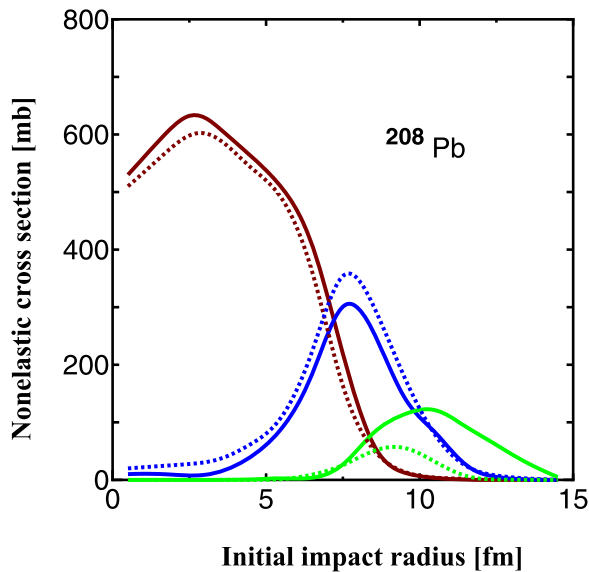
FIG. 9. Impact-parameter dependence of three different processes on the deuteron-induced nonelastic cross section: two-nucleon collision is shown in brown lines, single-particle transition process is in blue lines, and the breakup process is in green lines. Nonelastic cross sections of the three processes are the sum of their corresponding cross sections in a total reaction for a random distribution of the impact parameter, position, and angle of the incident deuteron. The incident energy of deuteron is taken at 100 MeV and the target is ^{208}Pb in this case.
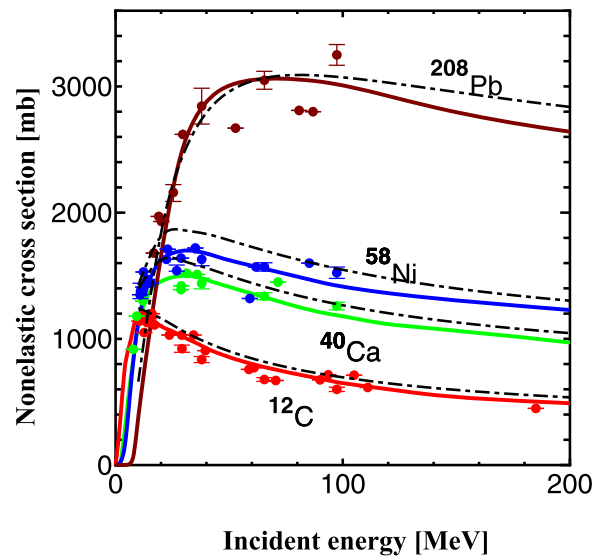

FIG. 10. Comparison of results obtained using empirical formula [31] (black dash-dotted lines) and INC model using Gaussian potential (solid lines) for deuteron-induced nonelastic cross sections of ^{12}C, ^{40}Ca, ^{58}Ni, and ^{208}Pb. The data points with error bars are experimental values.

an appreciable difference between the two potentials, which is similar to the difference between the Gaussian and the soft-core potentials in Fig. 4. The reason for this difference is mainly the decreased breakup reactions as shown in Fig. 9, which shows the impact-parameter dependence of three processes that occur in the injections. The three processes observed in this full set are (i) the two-nucleon collision (d, x), (ii) the sum of single-particle transition processes (d, px) and (d, nx), and (iii) breakup (d, pn), which involves no collision with the nucleons in the target. These processes are illustrated elsewhere [7].

Figure 9 shows clearly the place where the three processes occur frequently. Taking ^{208}Pb as an example, the two-nucleon collision occurs mostly in the central region (within 6 fm) and decreases sharply around the surface of the target, whereas the one-nucleon transition is concentrated on the surface of the target (around 7.5 fm), and breakup occurs outside the potential maximum radius (around 9 fm) where the sum of the Coulomb potential of the finite-size charge and nuclear potential with Wood-Saxon shape has its peak (which we call the ridge). The height of the ridge is 12.6 MeV in ^{208}Pb but less than half in ^{58}Ni (5.7 MeV), so the effects of the ridge are appreciable only for heavier nuclei such as ^{208}Pb. Breakup occurs when a deuteron strikes the ridge and is torn apart. When the two nucleons meet the ridge, the proton goes out because of the repulsive Coulomb potential and the neutron goes in the central region because of the attractive nuclear potential, thereby leading to breakup. Figure 9 also shows that the breakup process due to the soft-core potential is a slightly

smaller than that due to the Gaussian potential, especially in the region of large impact parameter. The reason for this decrease is the rotation of the two nucleons in the deuteron, which is essentially caused by the Coulomb potential: the two nucleons are more likely to rotate and hence escape the ridge for the soft-core potential.

Regarding which of the phenomenological potentials is better, the differences among them are within the experimental scatter as shown in Fig. 4, so it is difficult to determine which is better at reproducing the experimental data. However, a useful reference is an empirical expression for the deuteron-induced nonelastic cross section based on the continuum-discretized coupled-channels method [31]. As shown in Fig. 10, the empirically estimated values are slightly larger than the experimental values for ^{40}Ca and ^{56}Ni and those obtained with the Gaussian potential, thereby indicating the superiority of the Gaussian potential compared with soft-core potentials.

VI. CONCLUSIONS

Nonelastic cross sections are often discussed via an optical-potential approach, but in this study, we obtained them by explicitly considering the reaction processes based on the INC model. Here, the mutual proton-neutron potential is important for both the bounded size of the deuteron and describing the breakup or the one-nucleon transfer reaction.

In this paper, we investigated the differences among three mutual potentials of the deuteron for the deuteron-induced nonelastic cross sections of ^{12}C, ^{40}Ca, ^{58}Ni, and ^{208}Pb in the low-energy region below 200 MeV. First, we compared the results using the conventional Gaussian potential and two phenomenological soft-core potentials, namely, the Reid and Coester-Yen soft-core potentials, and we found that the

nonelastic cross sections obtained using both soft-core potentials were smaller than those obtained using the Gaussian potential, especially for ^{208}Pb. To investigate which part of the potential plays an important role, it was separated into two parts, namely, the potential tail in the outer region and the soft core in the central region. An important conclusion is that the Yukawa tail itself makes no appreciable difference for various targets below 200 MeV. This conclusion was deduced using a merging technique that causes a smooth transition from the Gaussian tail to the Yukawa tail. A more important conclusion is that soft-core potentials lead to decreased cross sections, especially for heavier nuclei such as ^{208}Pb. The reason for this decrease is the rotation of the two nucleons in the deuteron; this is essentially caused by the central repulsion, and thus this is a common feature of soft-core potentials.

Experimental and calculated nonelastic cross sections of ^{12}C, ^{40}Ca, ^{58}Ni, and ^{208}Pb in the low energy region below 200 MeV are compared. The experimental data were fairly well reproduced by all three phenomenological potentials. Interestingly, the three potentials used in quantum calculations also gave reasonable results for the classical INC model without any parameter adjustments. Although it is difficult to judge the optimal potential because the current experimental data are highly scattered, the cross sections obtained empirically [31] are closer to those obtained with the previously used Gaussian potential than to those obtained with the soft-core potentials.

[1] M. Nakano, Y. Yamaguchi, and Y. Uozumi, Phys. Rev. C **103**, 044608 (2021).

[2] M. Nakano and Y. Uozumi, Phys. Rev. C **100**, 034619 (2019).

[3] M. Nakano, Y. Yamaguchi, and Y. Uozumi, Phys. Rev. C **101**, 044616 (2020).

[4] M. Nakano, Y. Yamaguchi, and Y. Uozumi, Phys. Rev. C **102**, 024608 (2020).

[5] EXFOR: Experimental Nuclear Reaction Data (iaea.org), available from https://www-nds.iaea.org/exfor/ and references therein.

[6] J. W. Negele, Phys. Rev. C **1**, 1260 (1970).

[7] M. Nakano, Y. Yamaguchi, and Y. Uozumi, Phys. Rev. C **106**, 014612 (2022).

[8] R. V. Reid Jr., Ann. Phys. (N.Y.) **50**, 411 (1968).

[9] F. Coester and E. Yen, Nuovo Cimento **30**, 674 (1963).

[10] M. Lacombe, B. Loiseau, J. M. Richard, R. Vinh Mau, J. Côté, P. Pirès, and R. de Tourreil, Phys. Rev. C **21**, 861 (1980).

[11] V. G. J. Stoks, R. A. M. Klomp, C. P. F. Terheggen, and J. J. de Swart, Phys. Rev. C **49**, 2950 (1994).

[12] I. R. Afnan and B. F. Gibson, Phys. Rev. C **82**, 064002 (2010).

[13] R. Machleidt, K. Holinde, and Ch. Elster, Phys. Rep. **149**, 1 (1987).

[14] M. M. Nagels, T. A. Rijken, and J. J. de Swart, Phys. Rev. D **17**, 768 (1978).

[15] J. Haidenbauer and K. Holinde, Phys. Rev. C **40**, 2465 (1989).

[16] A. Boudard, J. Cugnon, J.-C. David, S. Leray, and D. Mancusi, Phys. Rev. C **87**, 014606 (2013).

[17] A. Boudard, J. Cugnon, S. Leray, and C. Volant, Phys. Rev. C **66**, 044615 (2002).

[18] T. E. Rodrigues, J. D. T. Arruda-Neto, A. Deppman, V. P. Likhachev, J. Mesa, C. Garcia, K. Shtejer, G. Silva, S. B. Duarte, and O. A. P. Tavares, Phys. Rev. C **69**, 064611 (2004).

[19] J. Cugnon, Th. Aoust, A. Boudard, J.-C. David, S. Pedoux. S. Leray, and Y. Yariv, Adv. Space Res. **40**, 1332 (2007).

[20] S. Pedoux and J. Cugnon, Nucl. Phys. A **866**, 16 (2011).

[21] D. Mancusi, A. Boudard, J. Cugnon, J.-C. David, P. Kaitaniemi, and S. Leray, Phys. Rev. C **90**, 054602 (2014).

[22] S. Furihata and T. Nakamura, J. Nucl. Sci. Technol. **39**, 758 (2002).

[23] Y. Uozumi, Y. Sawada, A. Mzhavia, S. Nogamine, H. Iwamoto, T. Kin, S. Hohara, G. Wakabayashi, and M. Nakano, Phys. Rev. C **84**, 064617 (2011).

[24] Y. Uozumi, T. Yamada, S. Nogamine, and M. Nakano, Phys. Rev. C **86**, 034610 (2012).

[25] Y. Uozumi, T. Yamada, and M. Nakano, J. Nucl. Sci. Technol. **52**, 264 (2015).

[26] M. J. Kobra, G. Watanabe, Y. Yamaguchi, Y. Uozumi, and M. Nakano, J. Nucl. Sci. Technol. **55**, 209 (2018).

[27] Y. Uozumi, Y. Yamaguchi, G. Watanabe, Y. Fukuda, R. Imamura, M. J. Kobra, and M. Nakano, Phys. Rev. C **97**, 034630 (2018).

[28] M. Avrigeanu and A. M. Moro, Phys. Rev. C **82**, 037601 (2010).

[29] M. Avrigeanu and V. Avrigeanu, Phys. Rev. C **92**, 021601(R) (2015).

[30] N. Ishii, S. Aoki, and T. Hatsuda, Phys. Rev. Lett. **99**, 022001 (2007).

[31] K. Minomo, K. Washiyama, and K. Ogata, J. Nucl. Sci. Technol. **54**, 127 (2017).